Polymer Chemistry

PAPER

View Article Online
View Journal | View Issue

Cite this: *Polym. Chem.*, 2015, **6**, 3054

Industrially-relevant polymerization-induced self-assembly formulations in non-polar solvents: RAFT dispersion polymerization of benzyl methacrylate†

Matthew J. Derry, Lee A. Fielding and Steven P. Armes*

Industrially-sourced mineral oil and a poly(α-olefin) are used as solvents for the reversible addition–fragmentation chain transfer (RAFT) dispersion polymerization of benzyl methacrylate (BzMA) using a poly(lauryl methacrylate) macromolecular chain transfer agent (PLMA macro-CTA) at 90 °C. The insolubility of the growing PBzMA chains under such conditions leads to polymerization-induced self-assembly (PISA), whereby poly(lauryl methacrylate)-poly(benzyl methacrylate) (PLMA-PBzMA) diblock copolymer spheres, worms or vesicles are produced directly as concentrated dispersions. The particular diblock copolymer composition required to access each individual morphology depends on the nature of the oil. Moreover, the solvent type also affects important properties of the physical free-standing gels that are formed by the PLMA-PBzMA worm dispersions, including the storage modulus (*G'*), critical gelation temperature (CGT) and critical gelation concentration (CGC). Spherical PLMA-PBzMA diblock copolymer nanoparticles can be prepared at up to 50% w/w solids and an efficient 'one-pot' protocol involving solution polymerization of LMA followed immediately by dispersion polymerization of BzMA has been developed. The latter formulation enables high BzMA conversions to be achieved, with spherical nanoparticles being produced at 30% w/w solids.

Received 2nd February 2015,
Accepted 2nd March 2015

DOI: 10.1039/c5py00157a

www.rsc.org/polymers

Introduction

Traditionally, block copolymer self-assembly in solution to form various types of nanoparticles is conducted at high dilution (<1% w/w) and often involves post-polymerization processing *via* solvent[1] or pH switching,[2] or thin film rehydration.[3] Over the last two decades or so, controlled radical techniques such as reversible addition–fragmentation chain transfer (RAFT) polymerization[4–6] have enabled the convenient synthesis of a wide range of functional diblock copolymers.[7–20] Currently, there is considerable academic interest in performing polymerization-induced self-assembly (PISA) syntheses at relatively high solids *via* RAFT dispersion polymerization.[21–24] The final diblock copolymer nanoparticle morphology typically depends on the relative volume fractions of the two blocks, as dictated by the so-called packing parameter,[25–27] and also the copolymer concentration.[28] Purely spherical, worm-like or vesicular morphologies have been reported for aqueous,[28–37] alcoholic[38–50] and non-polar[51–56] formulations, with the construction of phase diagrams enabling the reproducible targeting of each of these morphologies. Moreover, there appears to be some scope for developing 'one-pot' syntheses,[57–60] which should provide a highly convenient and potentially industrially-relevant protocol for generating organic nanoparticles.

A wide range of potential applications have been explored for selected RAFT PISA syntheses, including coatings,[61] drug delivery,[15,47,62] sterilizable gels,[63] contact lenses,[64] and novel Pickering emulsifiers.[65] In principle, block copolymer nanoparticles comprising an oil-soluble stabilizer such as poly(lauryl methacrylate) (PLMA) have various potential applications, including drag reduction,[66] oil absorbency agents,[67,68] and viscosity modifiers for engine oils.[69–71] Of particular relevance to the present work, Zheng *et al.*[72] reported that spherical block copolymer nanoparticles dispersed in non-polar solvents significantly reduced the friction coefficient of lubricant base oils in the boundary lubrication regime. In this case, copper-catalyzed atom transfer radical polymerization (ATRP) was utilized to synthesize all-acrylic block copolymer spheres in 2-butanone, with their subsequent redispersion in

Dainton Building, Department of Chemistry, The University of Sheffield, Brook Hill, Sheffield, South Yorkshire S3 7HF, UK. E-mail: s.p.armes@sheffield.ac.uk

†Electronic supplementary information (ESI) available: Table summarizing macro-CTAs; TEM evidence for different morphologies with the same diblock copolymer composition in each oil; DLS and TEM evidence for the worm-to-sphere transition of $PLMA_{18}$-$PBzMA_{40}$ worms upon heating to 90 °C; DLS size distribution of spheres synthesized *via* a 'one-pot' protocol. See DOI: 10.1039/c5py00157a

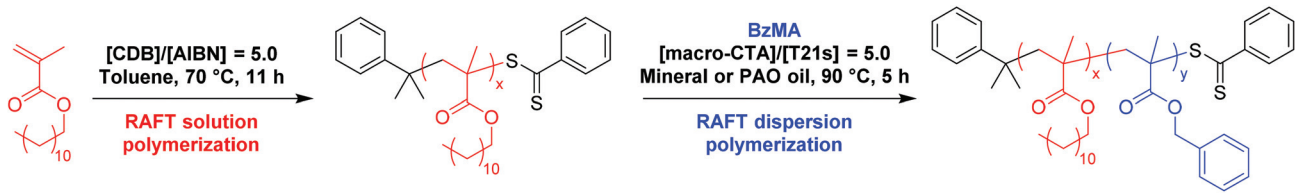

Fig. 1 Synthesis of a poly(lauryl methacrylate) macro-CTA *via* RAFT *solution* polymerization in toluene at 70 °C, followed by RAFT *dispersion* polymerization of benzyl methacrylate (BzMA) in mineral oil or a poly(α-olefin) (PAO) at 90 °C.

oil involving various post-polymerization modification and purification steps.[73]

Herein we revisit a RAFT-mediated dispersion polymerization formulation originally developed for the synthesis of poly(lauryl methacrylate)-poly(benzyl methacrylate) (PLMA-PBzMA) nanoparticles in *n*-alkanes and extend this formulation to include both mineral oil and a poly(α-olefin) (PAO) oil, see Fig. 1. Phase diagrams have been constructed for PISA syntheses conducted in both these industrially-sourced oils, and subtle differences are observed relative to pure *n*-alkanes, particularly with respect to the physical properties of PLMA-PBzMA worm gels. Moreover, a 'one-pot' synthesis protocol has been examined for the synthesis of spherical PLMA-PBzMA nanoparticles.

Experimental

Materials

Monomers were purchased from Sigma-Aldrich (UK) and passed through basic alumina prior to use. *tert*-Butyl peroxy-2-ethylhexanoate (T21s) initiator was purchased from AkzoNobel (The Netherlands). $CDCl_3$, cumyl dithiobenzoate (CDB) and all other reagents were purchased from Sigma-Aldrich (UK) and were used as received, unless otherwise noted. THF, *n*-heptane and toluene were purchased from Fisher Scientific (UK), CD_2Cl_2 was purchased from Goss Scientific (UK). Industrial-grade mineral (viscosity at 20 °C = 2.5 mPa s) and poly-(α-olefin) (PAO; viscosity at 20 °C = 3.0 mPa s) oils were provided by The Lubrizol Corporation Ltd.

Synthesis of poly(lauryl methacrylate) macro-chain transfer agent

The synthesis of poly(lauryl methacrylate) (PLMA) macro-CTAs has been previously reported.[54] A typical synthesis of a $PLMA_{47}$ macro-CTA was conducted as follows. A 250 mL round-bottomed flask was charged with lauryl methacrylate (LMA; 20.0 g; 78.6 mmol), cumyl dithiobenzoate (CDB; 0.43 g; 1.57 mmol; target degree of polymerization = 50), 2,2′-azobisisobutyronitrile (AIBN; 51.6 mg, 314 μmol; CDB/AIBN molar ratio = 5.0) and toluene (30.7 g). The sealed reaction vessel was purged with nitrogen and placed in a pre-heated oil bath at 70 °C for 11 h. The resulting PLMA (LMA conversion = 81%; M_n = 11 600 g mol^{-1}, M_w/M_n = 1.24) was purified by precipitation into excess methanol. The mean degree of polymerization (DP) of this macro-CTA was calculated to be 47 using ^{1}H NMR spectroscopy by comparing the integrated signals corresponding to the CDB aromatic protons at 7.1–8.1 ppm with that assigned to the two oxymethylene protons of PLMA at 3.7–4.2 ppm. Thus the CTA efficiency of the CDB was estimated to be 86%.

Synthesis of poly(lauryl methacrylate)-poly(benzyl methacrylate) diblock copolymer nanoparticles

A typical RAFT dispersion polymerization synthesis of $PLMA_{18}$-$PBzMA_{45}$ diblock copolymer nanoparticles at 25% w/w solids was carried out as follows. Benzyl methacrylate (BzMA; 0.415 g; 2.36 mmol), T21s initiator (2.26 mg; 10.5 μmol; dissolved at 10.0% v/v in mineral oil) and $PLMA_{18}$ macro-CTA (0.27 g; 52.3 μmol; macro-CTA/initiator molar ratio = 5.0; target degree of polymerization of PBzMA = 45) were dissolved in mineral oil (2.06 g). The reaction mixture was sealed in a 10 mL round-bottomed flask and purged with nitrogen gas for 30 min. The deoxygenated solution was then placed in a pre-heated oil bath at 90 °C for 5 h (final BzMA conversion = 99%; M_n = 9700 g mol^{-1}, M_w/M_n = 1.24).

'One-pot' synthesis of poly(lauryl methacrylate)-poly(benzyl methacrylate) diblock copolymer spheres

A typical 'one-pot' synthesis of $PLMA_{50}$-$PBzMA_{100}$ diblock copolymer spheres was conducted as follows. Lauryl methacrylate (LMA; 0.700 g; 2.75 mmol), cumyl dithiobenzoate (CDB; 15.0 mg; 55.0 μmol; target degree of polymerization = 50; dissolved at 10.0% w/w in mineral oil) and T21s initiator (2.14 mg; 9.90 μmol; dissolved at 10% v/v in mineral oil) were dissolved in mineral oil (0.150 g). The reaction mixture was sealed in a 25 mL round-bottomed flask and purged with nitrogen gas for 30 min. The deoxygenated solution was then placed in a pre-heated oil bath at 90 °C for 5 h (final LMA conversion = 95%; M_n = 12 500 g mol^{-1}; M_w/M_n = 1.18). Benzyl methacrylate (BzMA; 0.970 g; 5.50 mmol; target degree of polymerization = 100) and T21s initiator (2.14 mg; 9.90 μmol; dissolved at 10% v/v in mineral oil) were dissolved in mineral oil (3.65 g) and purged with nitrogen gas for 30 min before being added to the original reaction vessel at high (>95%) LMA conversion (final BzMA conversion = 98%; M_n = 24 500 g mol^{-1}; M_w/M_n = 1.15).

Gel permeation chromatography

Molecular weight distributions were assessed by gel permeation chromatography (GPC) using THF eluent. The THF GPC system was equipped with two 5 μm (30 cm) Mixed C

columns; a WellChrom K-2301 refractive index detector operating at 950 ± 30 nm. The mobile phase contained 2.0% v/v triethylamine and 0.05% w/v butylhydroxytoluene (BHT) with a toluene flow rate marker and the flow rate was fixed at 1.0 mL min^{-1}. A series of ten near-monodisperse poly(methyl methacrylate) standards (M_p values ranging from 1280 to 330 000 g mol^{-1}) were used for calibration.

^{1}H NMR spectroscopy

^{1}H NMR spectra were recorded in either CD_2Cl_2 or $CDCl_3$ using a Bruker AV1-400 or AV1-250 MHz spectrometer. Typically 64 scans were averaged per spectrum.

Dynamic light scattering

Dynamic light scattering (DLS) studies were performed using a Zetasizer Nano-ZS instrument (Malvern Instruments, UK) at a fixed scattering angle of 173°. Copolymer dispersions were diluted in *n*-heptane (0.10% w/w) prior to light scattering studies at 25 °C. Temperature-dependent DLS studies were performed using the same Zetasizer Nano-ZS instrument, which was equipped with a Peltier cell. Copolymer dispersions were diluted in *n*-heptane and heated from 20 to 90 °C at 5 °C intervals allowing 5 min for thermal equilibration between measurements. In both sets of experiments, the intensity-average diameter and polydispersity of the diblock copolymer particles were calculated by cumulants analysis of the experimental correlation function using Dispersion Technology Software version 6.20. Data were averaged over thirteen runs each of thirty seconds duration.

Transmission electron microscopy

Transmission electron microscopy (TEM) studies were conducted using a Philips CM 100 instrument operating at 100 kV and equipped with a Gatan 1 k CCD camera. Diluted block copolymer solutions (0.10% w/w) were placed on carbon-coated copper grids and exposed to ruthenium(VIII) oxide vapor for 7 minutes at 20 °C prior to analysis.[74] This heavy metal compound acted as a positive stain for the core-forming PBzMA block to improve contrast. The ruthenium(VIII) oxide was prepared as follows: ruthenium(IV) oxide (0.30 g) was added to water (50 g) to form a black slurry; addition of sodium periodate (2.0 g) with stirring produced a yellow solution of ruthenium(VIII) oxide within 1 min.[75]

Rheology measurements

An AR-G2 rheometer equipped with a variable temperature Peltier plate and a 40 mm 2° aluminum cone was used for all experiments. The loss and storage moduli were measured as a function of temperature at a heating rate of 1.0 °C per minute, a fixed strain of 1.0% and an angular frequency of 10 rad s^{-1} so as to assess the gel strength and critical gelation temperature (CGT). During temperature sweeps, the temperature was varied at 5 °C intervals, with an equilibration time of five minutes being allowed prior to each measurement. In all cases the gap between the cone and plate was 58 μm.

Results and discussion

Synthesis of PLMA macro-CTAs

Low-polydispersity PLMA macro-CTAs with mean DPs of 16, 18, or 47 (see Table S1 in ESI†) were synthesized *via* RAFT solution polymerization in toluene at 70 °C using cumyl dithiobenzoate (CDB) as a CTA. In all macro-CTA syntheses, the polymerization was quenched at 71–81% conversion in order to avoid monomer-starved conditions and therefore ensure retention of the RAFT end-groups.[76,77] This is usually considered to be desirable for high blocking efficiencies and hence well-defined PLMA-PBzMA diblock copolymers. As with previous studies reporting well-controlled RAFT syntheses conducted in non-polar solvents,[54,55] each PLMA macro-CTA had a polydispersity (M_w/M_n) of less than 1.25. A representative kinetic study of the RAFT solution polymerization of LMA to prepare a $PLMA_{18}$ macro-CTA indicated a linear evolution of molecular weight with conversion (see Fig. S1 in ESI†). After an initial induction period of ~100 min, this reaction obeyed first-order kinetics and was quenched after 11 h (71% conversion).

PLMA-PBzMA block copolymer syntheses and phase diagrams

One important trend in the commercial engine oil sector is a general shift from mineral oil towards wholly synthetic oils such as poly(α-olefins). Preliminary experiments confirmed that both these industrially-sourced solvents were good solvents for PLMA and bad solvents for PBzMA. Hence phase diagrams for PLMA-PBzMA block copolymer nanoparticles prepared in these two oils were constructed in order to assess the effect of the nature of the solvent on the positions of the phase boundaries. Firstly, BzMA monomer was polymerized using a low-polydispersity $PLMA_{18}$ macro-CTA *via* RAFT dispersion polymerization in mineral oil to produce a series of well-defined PLMA-PBzMA diblock copolymer nanoparticles at various copolymer concentrations. More than 95% BzMA conversion was achieved in all dispersion polymerizations within 5 h at 90 °C, as judged by ^{1}H NMR spectroscopy. Pure spherical, worm-like, or vesicular morphologies (as judged by TEM) can be accessed when chain-extending the $PLMA_{18}$ macro-CTA (see Fig. 2a, b and c, respectively). We have previously reported phase diagrams for PLMA-PBzMA diblock copolymer formulations in *n*-heptane[54] and *n*-dodecane.[55] Pure spherical and vesicular phases were obtained at copolymer concentrations ranging from 12.5 to 25% w/w, whereas solely worm-like micelles could only be obtained at copolymer concentrations at or above 18% w/w. At first sight, the phase diagram reported in the present work (Fig. 2) is similar to that reported for *n*-heptane, but the precise block copolymer compositions required to access each individual morphology are subtly different. This shift in phase boundaries is best highlighted when comparing the pure worm phase in each oil. In *n*-heptane, the worm phase for $PLMA_{17}$-$PBzMA_x$ diblock copolymers corresponds to $x \approx 50$–70, whereas worms are obtained at $x \approx 37$–47 for a $PLMA_{18}$-$PBzMA_x$ formulation in mineral oil

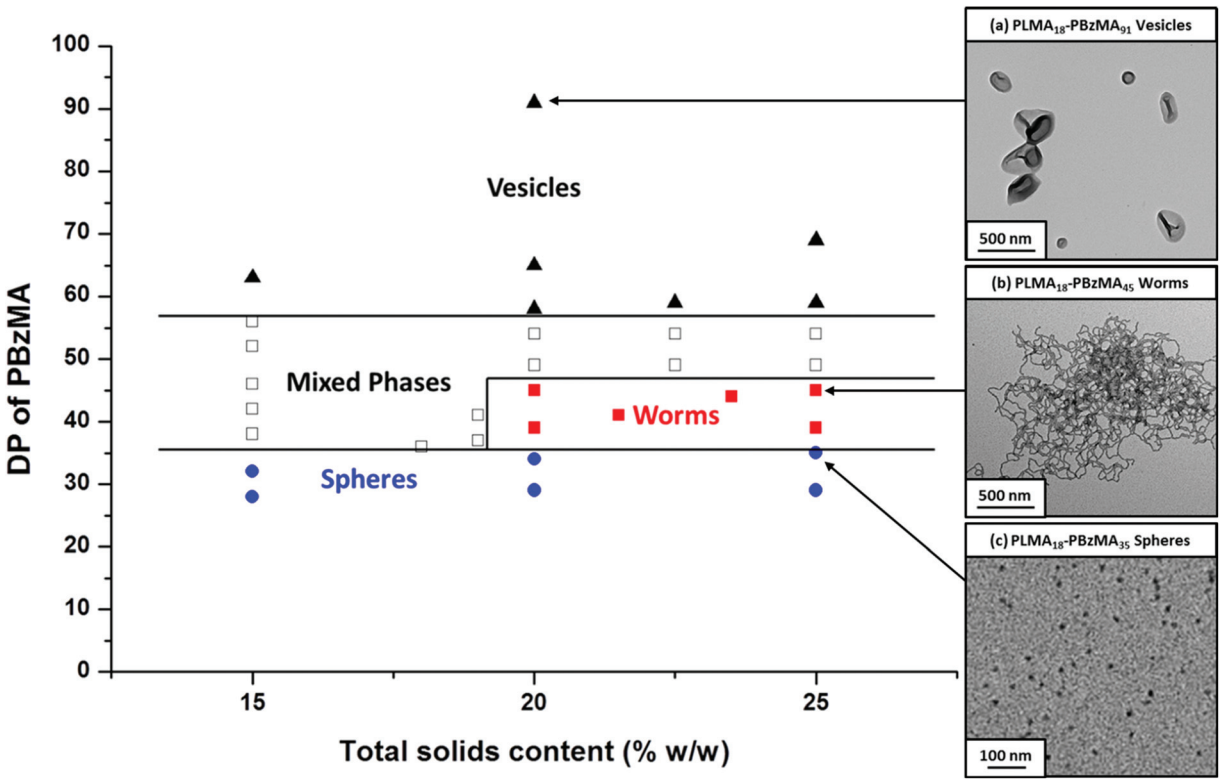

Fig. 2 Phase diagram constructed for $PLMA_{18}$-$PBzMA_x$ diblock copolymer nanoparticles prepared by RAFT dispersion polymerization of BzMA in mineral oil using T21s initiator at 90 °C ([PLMA]/[T21s] = 5.0). The *post mortem* diblock copolymer morphologies were assigned by TEM studies. TEM images (a), (b) and (c) represent examples of purely vesicular, worm-like or spherical morphologies, respectively.

(see Fig. 2), which is close to that observed for *n*-dodecane (x = 36–44).[55]

Evaluation of the effect of solvent on PLMA-PBzMA worm gels

Using an industrially-sourced PAO as the continuous phase for the synthesis of PLMA-PBzMA diblock copolymer nano-objects enables the role of the solvent in such PISA syntheses to be examined. Accordingly, a $PLMA_{16}$ macro-CTA was chain-extended with varying amounts of BzMA at various solids contents in order to construct a phase diagram (Fig. 3). Although this exhibits obvious similarities to the phase diagram obtained for $PLMA_{18}$-$PBzMA_x$ in mineral oil (Fig. 2), nevertheless some differences are observed. In particular, for $PLMA_{16}$-$PBzMA_x$ syntheses conducted at ≥20% w/w solids, the PAO worm phase is observed for $x \approx 28$–35. In contrast, the worm phase obtained for $PLMA_{18}$-$PBzMA_x$ when using mineral oil occurs for $x \approx 37$–47. Even allowing for the small differences between the mean DPs of the PLMA stabilizer blocks, it is clear that a somewhat longer PBzMA block is required to access the worm phase in mineral oil. This suggests that PAO is a slightly poorer solvent for the growing PBzMA chains than the mineral oil. In order to further illustrate this point, $PLMA_{18}$-$PBzMA_{45}$ nano-objects were prepared at 20% w/w solids in both PAO and mineral oil (see Fig. S2 in ESI†). Inspecting Fig. 2, $PLMA_{18}$-$PBzMA_{45}$ forms a pure worm phase in the latter solvent. However, *precisely the same diblock copolymer composition* forms a mixed phase of spheres, worms and vesicles in PAO (Fig. S2†). In view of these subtle solvent effects, the physical properties of free-standing worm gels prepared in *n*-dodecane,[55] mineral oil and PAO oil were compared *via* rheology (Table 1).

PLMA-PBzMA worm gels in the mineral and PAO oils provided G' values that are approximately an order of magnitude greater than in *n*-dodecane. This suggests that the worms are either significantly longer and/or that there are stronger inter-worm interactions in these gels. The G' for the 20% w/w $PLMA_{16}$-$PBzMA_{32}$ worm gel in PAO oil is significantly greater than that of the $PLMA_{18}$-$PBzMA_{45}$ worm gel in mineral oil. The critical gelation temperature (CGT) of worm gels is defined as the temperature at which the dispersion no longer forms a gel (*i.e.* when $G'' > G'$).[78] In our previous study,[55] we found that a worm-to-sphere transition was responsible for the degelation of such worm gels above the CGT. The same morphological transition is believed to be responsible for the degelation that occurs on heating in the present study. This hypothesis is supported by TEM and DLS studies (see Fig. S3 in ESI†). Thus the sphere-equivalent particle diameter of 163 nm (polydispersity = 0.39) obtained for the initial $PLMA_{18}$-$PBzMA_{40}$ worms formed in mineral oil is reduced to 28 nm (polydispersity = 0.10) for spheres on heating to 90 °C. For PLMA-PBzMA worm gels prepared in the three oils, the CGT ranged from 44 to 49 °C. Interestingly, the $PLMA_{16}$-$PBzMA_{32}$ worm gel produced

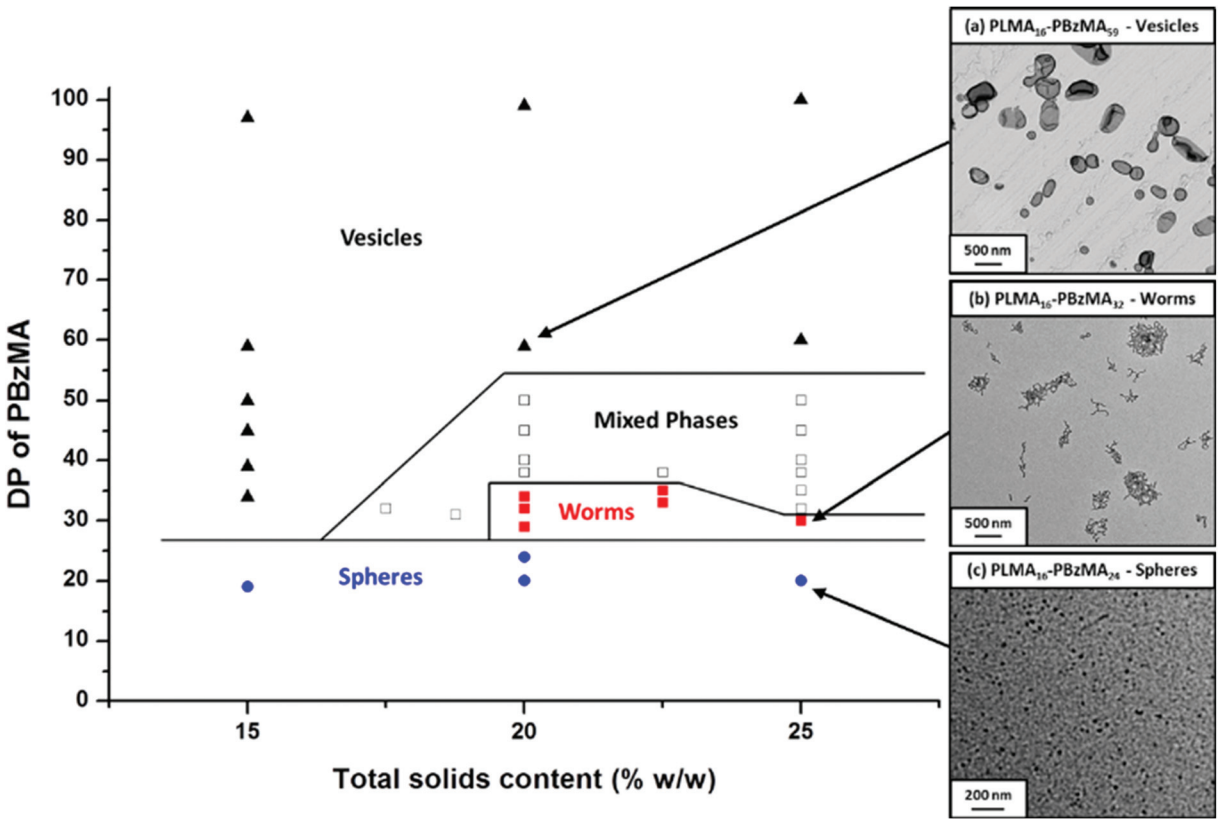

Fig. 3 Phase diagram constructed for $PLMA_{16}$-$PBzMA_x$ diblock copolymer nanoparticles prepared by RAFT dispersion polymerization of BzMA in poly(α-olefin) oil using T21s initiator at 90 °C ([PLMA]/[T21s] = 5.0). The *post mortem* diblock copolymer morphologies were assigned by TEM studies. TEM images (a), (b) and (c) represent examples of pure vesicular, worm-like or spherical morphologies, respectively.

Table 1 Summary of physical properties of 20% w/w PLMA-PBzMA worm gels prepared in various non-polar solvents: initial storage modulus (G') at 20 °C, critical gelation temperature (CGT) and critical gelation concentration (CGC). Measurements were obtained at a heating rate of 1.0 °C min^{-1}, a fixed strain of 1.0% and an angular frequency of 10 rad s^{-1}. The temperature was varied at 5 °C intervals, with a 5 min equilibration time at each temperature

Solvent	Block composition	Initial G' at 20 °C/Pa	CGT/°C	CGC/ % w/w
n-Dodecane[55]	$PLMA_{18}$-$PBzMA_{37}$	2300	47	~11
Mineral oil	$PLMA_{18}$-$PBzMA_{45}$	21 000	49	9
PAO oil	$PLMA_{16}$-$PBzMA_{32}$	41 000	44	9

in PAO oil, which provided the highest G', possessed the lowest CGT. The specific DP of the PBzMA core-forming block may influence this parameter, since higher CGTs are observed for longer core-forming PBzMA blocks for the three worm gels characterized in this study. The dispersion is a free-flowing fluid below the critical gelation concentration (CGC), which is slightly lower for the industrially-sourced oils than for *n*-dodecane. However, all of the non-polar worm gels investigated in the present work exhibit much higher CGCs than previously reported *aqueous* worm gels.[78] This might perhaps reflect the lack of inter-worm hydrogen bonding in the non-aqueous formulations.

Synthesis of PLMA-PBzMA diblock copolymer spheres at high solids

In many RAFT dispersion polymerization formulations, it has been reported that only spherical nanoparticles are obtained when chain-extending a sufficiently long macro-CTA.[42,54,55] This is presumably because inter-sphere fusion must first occur if a so-called 'higher order' non-spherical morphology (such as worms) is to be generated. Thus using a longer steric stabilizer block confers more effective steric stabilization, which inevitably leads to a higher proportion of elastic inter-particle collisions. Using a $PLMA_{47}$ macro-CTA is sufficient to ensure an exclusively spherical morphology for all $PLMA_{47}$-$PBzMA_x$ diblock copolymers prepared by RAFT dispersion polymerization in mineral oil, regardless of the targeted degree of polymerization (x). For example, well-defined spherical nanoparticles are obtained for both $PLMA_{47}$-$PBzMA_{99}$ and $PLMA_{47}$-$PBzMA_{495}$ diblock copolymer nanoparticles prepared at 20% w/w solids. This copolymer concentration allows access to pure worm-like and vesicular morphologies when using shorter PLMA macro-CTAs.[54,55] $PLMA_{47}$-$PBzMA_{495}$ diblock copolymer spheres are significantly larger than $PLMA_{47}$-$PBzMA_{99}$,

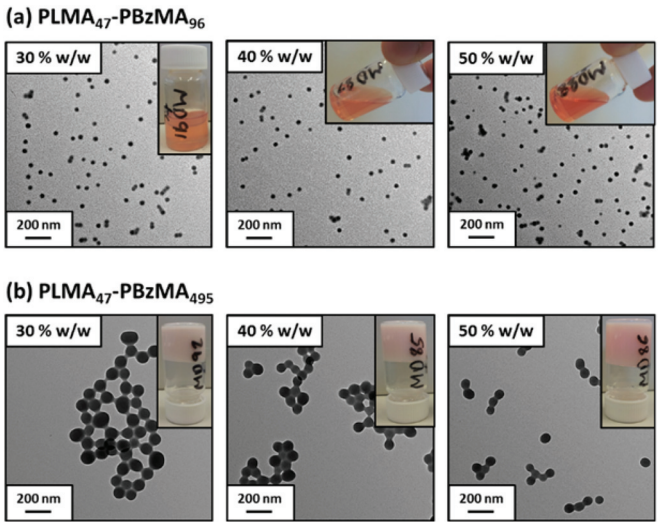

Fig. 4 (a) $PLMA_{47}$-$PBzMA_{99}$ and (b) $PLMA_{47}$-$PBzMA_{495}$ diblock copolymer spheres prepared *via* RAFT dispersion polymerization of benzyl methacrylate at 90 °C using PISA formulations conducted at 30, 40 or 50% w/w solids. Inset digital photos depict physical appearance of each dispersion.

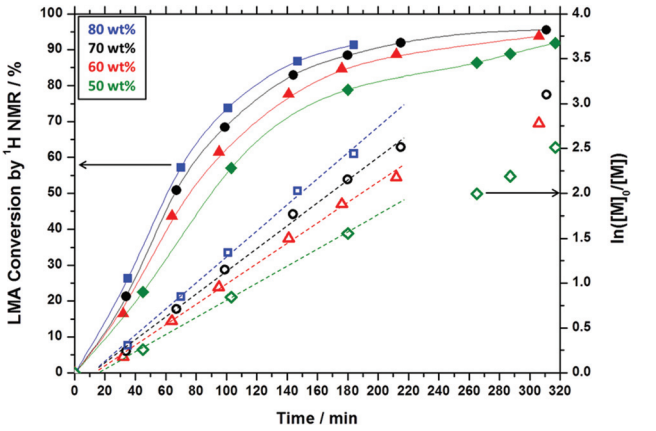

Fig. 5 Kinetic data obtained for the RAFT solution polymerization of a $PLMA_{50}$ macro-CTA in mineral oil at 90 °C conducted at 50 (green diamonds), 60 (red triangles), 70 (black circles) and 80 (blue squares) % w/w solids using CDB as a RAFT chain transfer agent and T21s initiator.

as confirmed by TEM (Fig. 4). Given the diblock copolymer asymmetry, the former particles most likely represent a kinetically-trapped morphology.[35,79] Interestingly, such spherical nanoparticles can be synthesized at copolymer concentrations up to 50% w/w, with the smaller $PLMA_{47}$-$PBzMA_{99}$ spheres producing a viscous free-flowing dispersion. The synthesis of relatively small spherical nanoparticles at high solids bodes well for the industrial relevance of such PISA formulations. In contrast, the larger $PLMA_{47}$-$PBzMA_{495}$ spheres lead to stirring problems at concentrations as low as 30% w/w solids, with a gel-like paste being obtained (see Fig. 4b, inset digital images).

'One-pot' synthesis of PLMA-PBzMA spheres at high solids

To further examine the robust nature (and hence potential industrial relevance) of this particular PISA formulation, a series of 'one-pot' polymerizations were conducted in mineral oil. Firstly, a kinetic study of the RAFT solution polymerization of LMA in mineral oil was conducted (Fig. 5). Efficient polymerizations could be conducted at up to 70% w/w solids when targeting a $PLMA_{50}$ macro-CTA: a linear semi-logarithmic plot indicated first-order kinetics up to 90% LMA conversion. At 80% w/w solids, the solution viscosity became too high for efficient stirring above 90% LMA conversion, but similar first-order polymerization kinetics were observed up to this point. As expected, polymerizations conducted at higher LMA concentrations exhibited faster rates of polymerization, with conversions reaching 90% within 180 min at 80% w/w, 220 min at 70% w/w, 300 min at 60% w/w, and >320 min at 50% w/w. The homopolymerization of LMA conducted at 70% w/w reached high (>95%) conversion within 320 min. Moreover, this reaction solution remained sufficiently fluid for efficient stirring. Hence these conditions were selected for the first stage of a 'one-pot' synthesis of $PLMA_{50}$-$PBzMA_{100}$ diblock copolymer nanoparticles. The subsequent RAFT dispersion polymerization of BzMA was conducted at 30% w/w solids in order to enable the reaction mixture to be efficiently stirred throughout the polymerization. We had previously observed that similar $PLMA_{47}$-$PBzMA_{99}$ block copolymer spheres prepared *via* a traditional two-step synthesis exhibited relatively high viscosities above 30% w/w solids, see Fig. 4. Kinetic data were obtained for both the RAFT solution polymerization of LMA at 70% w/w solids and the RAFT dispersion polymerization of BzMA at 30% w/w solids in mineral oil (Fig. 6). A degassed solution of BzMA in mineral oil containing additional T21s initiator was added to the reaction mixture once the LMA conversion had reached 95%. Initially, a relatively slow rate of BzMA polymerization was observed for the first 40 min until a critical degree of polymerization of the growing PBzMA chains is reached, at which point micellar nucleation occurred (see stage (b) in Fig. 6). Thereafter, the polymerization proceeds much faster, because the unreacted BzMA migrates into the PBzMA micelle cores, thus producing a relatively high local monomer concentration as suggested by Blanazs *et al.*[33] Thereafter, first-order kinetics was observed from 30 to 90% conversions (see Fig. 6). The final diblock copolymer spheres were relatively monodisperse with an intensity-average diameter of 39 nm, as judged by DLS (see Fig. S4 in ESI†). Molecular weight distributions for each of the data points shown in Fig. 6 were assessed using GPC (Fig. 7a). A linear evolution in number-average molecular weight (expressed in poly(methyl methacrylate) equivalents) was observed for both solution and dispersion polymerizations (Fig. 7b), with relatively narrow molecular weight distributions (M_w/M_n < 1.20) being achieved throughout both polymerizations. Thus excellent RAFT control can be achieved in such 'one-pot' syntheses.

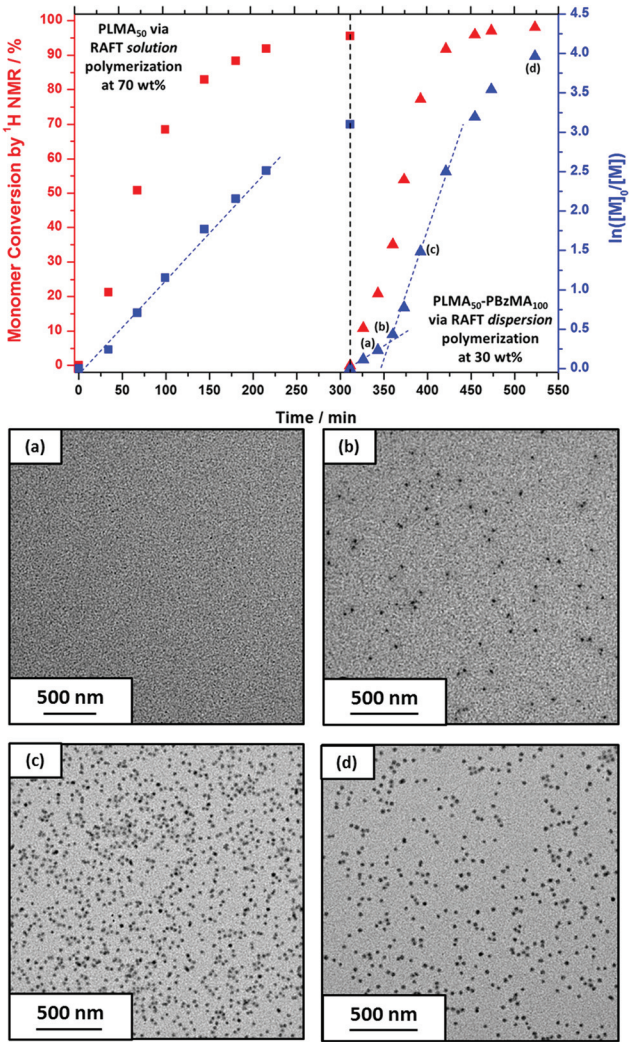

Fig. 6 Conversion *vs.* time curves obtained for the 'one-pot' synthesis of $PLMA_{50}$-$PBzMA_{100}$ diblock copolymer spheres in mineral oil: RAFT solution polymerization of a $PLMA_{50}$ macro-CTA at 70% w/w solids (squares) followed by the RAFT dispersion polymerization of BzMA at 30% w/w solids (triangles). BzMA was added after 310 min. TEM images (a), (b), (c), and (d) represent various points in the kinetic data and indicate the onset of micellization at (b).

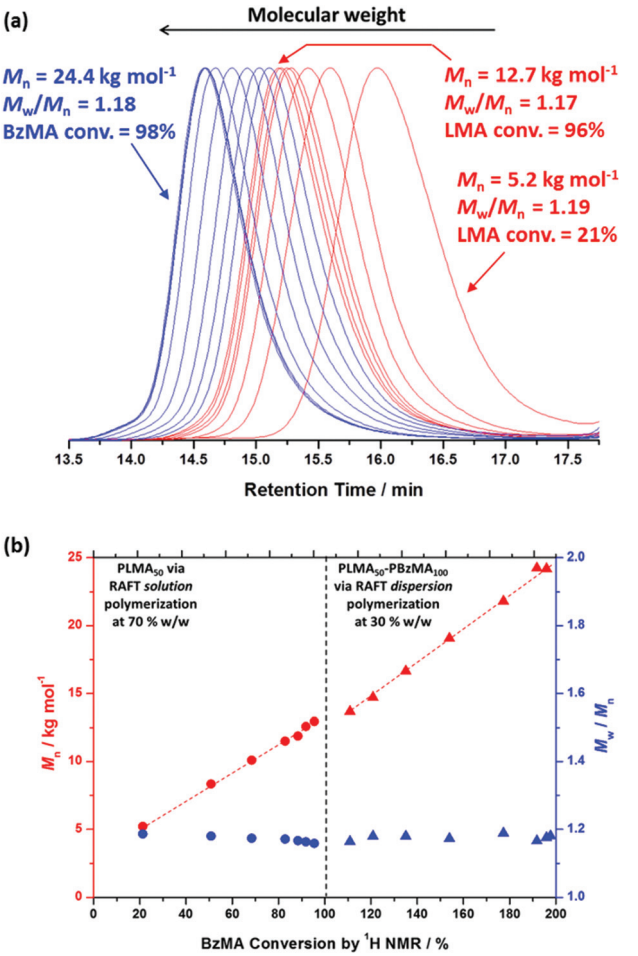

Fig. 7 (a) THF gel permeation chromatograms (*vs.* poly(methyl methacrylate) standards) obtained for the 'one-pot' synthesis of $PLMA_{50}$-$PBzMA_{100}$ diblock copolymer spheres in mineral oil: *solution* polymerization of LMA (red traces) and *dispersion* polymerization of BzMA (blue traces). (b) Number-average molecular weight *vs.* monomer conversion plots for the RAFT *solution* polymerization of LMA at 70% w/w solids (circles) and the subsequent RAFT *dispersion* polymerization of BzMA at 30% w/w solids in mineral oil (triangles).

Conclusions

In summary, well-defined PLMA-PBzMA block copolymer nano-objects can be reproducibly prepared in the form of spheres, worms and vesicles *via* polymerization-induced self-assembly in industrially-sourced mineral oil at 90 °C, provided that the mean degree of polymerization of the PLMA stabilizer block is sufficiently low (*e.g.*, DP = 18). The phase diagram constructed for $PLMA_{18}$-$PBzMA_x$ diblock copolymers in mineral oil is very similar to that previously reported for *n*-dodecane.[55] However, subtle variation in the precise location of phase boundaries is observed for $PLMA_{16}$-$PBzMA_x$ diblock copolymers in a second industrially-relevant solvent, poly(α-olefin) (PAO) oil. The nature of the oil also affected the physical properties of the worm gels, with a worm gel in PAO oil exhibiting a higher storage modulus (G') than those in mineral oil and *n*-dodecane. The critical gelation temperature (CGT) for each worm gel was found to be 44–49 °C, with the strongest worm gel (in PAO oil) having the lowest CGT. The critical gelation concentration (CGC) was lower for PLMA-PBzMA worm gels synthesized in the industrially-sourced oils compared to those previously studied in *n*-dodecane. Purely spherical nanoparticles are obtained when using a PLMA stabilizer with a relatively high DP. In this case, PISA syntheses can be conducted at up to 50% w/w solids when targeting $PLMA_{47}$-$PBzMA_{100}$, with efficient stirring being maintained throughout the polymerization. A convenient 'one-pot' synthesis protocol has also been explored. Thus the PLMA macro-CTA is first synthesized at 70% w/w solids in mineral oil *via* RAFT solution polymerization, with subsequent chain extension *via* RAFT dis-

persion polymerization of BzMA being conducted at 30% w/w solids. The final $PLMA_{50}$-$PBzMA_{100}$ spherical nanoparticles were obtained at 98% conversion with a relatively narrow size distribution, as judged by TEM and DLS studies. Moreover, relatively high blocking efficiencies and low final copolymer polydispersities ($M_w/M_n < 1.20$) were indicated by GPC studies.

Acknowledgements

The EPSRC (EP/J007846/1) is thanked for providing post-doctoral support for LAF. SPA also acknowledges an ERC Advanced Investigator grant (PISA 320372).

Notes and references

1 L. F. Zhang and A. Eisenberg, *Science*, 1995, **268**, 1728–1731.
2 V. Bütün, S. P. Armes and N. C. Billingham, *Polymer*, 2001, **42**, 5993–6008.
3 J. R. Howse, R. A. L. Jones, G. Battaglia, R. E. Ducker, G. J. Leggett and A. J. Ryan, *Nat. Mater.*, 2009, **8**, 507–511.
4 J. Chiefari, Y. K. Chong, F. Ercole, J. Krstina, J. Jeffery, T. P. T. Le, R. T. A. Mayadunne, G. F. Meijs, C. L. Moad, G. Moad, E. Rizzardo and S. H. Thang, *Macromolecules*, 1998, **31**, 5559–5562.
5 G. Moad, E. Rizzardo and S. H. Thang, *Aust. J. Chem.*, 2005, **58**, 379–410.
6 G. Moad, E. Rizzardo and S. H. Thang, *Acc. Chem. Res.*, 2008, **41**, 1133–1142.
7 Y. Mitsukami, M. S. Donovan, A. B. Lowe and C. L. McCormick, *Macromolecules*, 2001, **34**, 2248–2256.
8 A. B. Lowe, B. S. Sumerlin, M. S. Donovan and C. L. McCormick, *J. Am. Chem. Soc.*, 2002, **124**, 11562–11563.
9 C. Barner-Kowollik, T. P. Davis, J. P. A. Heuts, M. H. Stenzel, P. Vana and M. Whittaker, *J. Polym. Sci., Part A: Polym. Chem.*, 2003, **41**, 365–375.
10 S. Perrier and P. Takolpuckdee, *J. Polym. Sci., Part A: Polym. Chem.*, 2005, **43**, 5347–5393.
11 M. Mertoglu, S. Garnier, A. Laschewsky, K. Skrabania and J. Storsberg, *Polymer*, 2005, **46**, 7726–7740.
12 D. Quémener, T. P. Davis, C. Barner-Kowollik and M. H. Stenzel, *Chem. Commun.*, 2006, 5051–5053.
13 A. B. Lowe and C. L. McCormick, *Prog. Polym. Sci.*, 2007, **32**, 283–351.
14 C. Barner-Kowollik and S. Perrier, *J. Polym. Sci., Part A: Polym. Chem.*, 2008, **46**, 5715–5723.
15 C. Boyer, V. Bulmus, T. P. Davis, V. Ladmiral, J. Q. Liu and S. Perrier, *Chem. Rev.*, 2009, **109**, 5402–5436.
16 A. E. Smith, X. Xu and C. L. McCormick, *Prog. Polym. Sci.*, 2010, **35**, 45–93.
17 R. K. O'Reilly, *Polym. Int.*, 2010, **59**, 568–573.
18 C. Boyer, M. H. Stenzel and T. P. Davis, *J. Polym. Sci., Part A: Polym. Chem.*, 2011, **49**, 551–595.
19 A. Lu, T. P. Smart, T. H. Epps, D. A. Longbottom and R. K. O'Reilly, *Macromolecules*, 2011, **44**, 7233–7241.
20 Y. Kang, A. Pitto-Barry, H. Willcock, W. D. Quan, N. Kirby, A. M. Sanchez and R. K. O'Reilly, *Polym. Chem.*, 2015, **6**, 106–117.
21 B. Charleux, G. Delaittre, J. Rieger and F. D'Agosto, *Macromolecules*, 2012, **45**, 6753–6765.
22 M. J. Monteiro and M. F. Cunningham, *Macromolecules*, 2012, **45**, 4939–4957.
23 J.-T. Sun, C.-Y. Hong and C.-Y. Pan, *Polym. Chem.*, 2013, **4**, 873–881.
24 N. J. Warren and S. P. Armes, *J. Am. Chem. Soc.*, 2014, **136**, 10174–10185.
25 J. N. Israelachvili, D. J. Mitchell and B. W. Ninham, *J. Chem. Soc., Faraday Trans.*, 1976, **72**, 1525–1568.
26 M. Antonietti and S. Förster, *Adv. Mater.*, 2003, **15**, 1323–1333.
27 A. Blanazs, S. P. Armes and A. J. Ryan, *Macromol. Rapid Commun.*, 2009, **30**, 267–277.
28 S. Sugihara, A. Blanazs, S. P. Armes, A. J. Ryan and A. L. Lewis, *J. Am. Chem. Soc.*, 2011, **133**, 15707–15713.
29 Z. An, Q. Shi, W. Tang, C.-K. Tsung, C. J. Hawker and G. D. Stucky, *J. Am. Chem. Soc.*, 2007, **129**, 14493–14499.
30 J. Rieger, C. Grazon, B. Charleux, D. Alaimo and C. Jérôme, *J. Polym. Sci., Part A: Polym. Chem.*, 2009, **47**, 2373–2390.
31 S. Boisse, J. Rieger, K. Belal, A. Di-Cicco, P. Beaunier, M.-H. Li and B. Charleux, *Chem. Commun.*, 2010, **46**, 1950–1952.
32 Y. Li and S. P. Armes, *Angew. Chem., Int. Ed.*, 2010, **49**, 4042–4046.
33 A. Blanazs, J. Madsen, G. Battaglia, A. J. Ryan and S. P. Armes, *J. Am. Chem. Soc.*, 2011, **133**, 16581–16587.
34 G. Liu, Q. Qiu, W. Shen and Z. An, *Macromolecules*, 2011, **44**, 5237–5245.
35 A. Blanazs, A. J. Ryan and S. P. Armes, *Macromolecules*, 2012, **45**, 5099–5107.
36 N. J. Warren, O. O. Mykhaylyk, D. Mahmood, A. J. Ryan and S. P. Armes, *J. Am. Chem. Soc.*, 2014, **136**, 1023–1033.
37 C. A. Figg, A. Simula, K. A. Gebre, B. S. Tucker, D. M. Haddleton and B. S. Sumerlin, *Chem. Sci.*, 2015, **6**, 1230–1236.
38 W.-M. Wan and C.-Y. Pan, *Polym. Chem.*, 2010, **1**, 1475–1484.
39 W.-M. Wan, X.-L. Sun and C.-Y. Pan, *Macromol. Rapid Commun.*, 2010, **31**, 399–404.
40 C.-Q. Huang and C.-Y. Pan, *Polymer*, 2010, **51**, 5115–5121.
41 W. Cai, W. Wan, C. Hong, C. Huang and C. Pan, *Soft Matter*, 2010, **6**, 5554–5561.
42 E. R. Jones, M. Semsarilar, A. Blanazs and S. P. Armes, *Macromolecules*, 2012, **45**, 5091–5098.
43 M. Semsarilar, E. R. Jones, A. Blanazs and S. P. Armes, *Adv. Mater.*, 2012, **24**, 3378–3382.
44 M. Semsarilar, V. Ladmiral, A. Blanazs and S. P. Armes, *Polym. Chem.*, 2014, **5**, 3466–3475.

45 C. Gonzato, M. Semsarilar, E. R. Jones, F. Li, G. J. P. Krooshof, P. Wyman, O. O. Mykhaylyk, R. Tuinier and S. P. Armes, *J. Am. Chem. Soc.*, 2014, **136**, 11100–11106.
46 Y. Pei and A. B. Lowe, *Polym. Chem.*, 2014, **5**, 2342–2351.
47 B. Karagoz, L. Esser, H. T. Duong, J. S. Basuki, C. Boyer and T. P. Davis, *Polym. Chem.*, 2014, **5**, 350–355.
48 B. Karagoz, C. Boyer and T. P. Davis, *Macromol. Rapid Commun.*, 2014, **35**, 417–421.
49 W. Zhao, G. Gody, S. M. Dong, P. B. Zetterlund and S. Perrier, *Polym. Chem.*, 2014, **5**, 6990–7003.
50 S. Dong, W. Zhao, F. P. Lucien, S. Perrier and P. B. Zetterlund, *Polym. Chem.*, 2015, DOI: 10.1039/C4PY01632G.
51 L. Houillot, C. Bui, M. Save, B. Charleux, C. Farcet, C. Moire, J.-A. Raust and I. Rodriguez, *Macromolecules*, 2007, **40**, 6500–6509.
52 L. Houillot, C. Bui, C. Farcet, C. Moire, J.-A. Raust, H. Pasch, M. Save and B. Charleux, *ACS Appl. Mater. Interfaces*, 2010, **2**, 434–442.
53 J. A. Raust, L. Houillot, M. Save, B. Charleux, C. Moire, C. Farcet and H. Pasch, *Macromolecules*, 2010, **43**, 8755–8765.
54 L. A. Fielding, M. J. Derry, V. Ladmiral, J. Rosselgong, A. M. Rodrigues, L. P. D. Ratcliffe, S. Sugihara and S. P. Armes, *Chem. Sci.*, 2013, **4**, 2081–2087.
55 L. A. Fielding, J. A. Lane, M. J. Derry, O. O. Mykhaylyk and S. P. Armes, *J. Am. Chem. Soc.*, 2014, **136**, 5790–5798.
56 Y. Pei, L. Thurairajah, O. R. Sugita and A. B. Lowe, *Macromolecules*, 2015, **48**, 236–244.
57 I. Chaduc, W. J. Zhang, J. Rieger, M. Lansalot, F. D'Agosto and B. Charleux, *Macromol. Rapid Commun.*, 2011, **32**, 1270–1276.
58 L. P. D. Ratcliffe, A. J. Ryan and S. P. Armes, *Macromolecules*, 2013, **46**, 769–777.
59 W. Zhang, F. D'Agosto, P.-Y. Dugas, J. Rieger and B. Charleux, *Polymer*, 2013, **54**, 2011–2019.
60 L. Guo, Y. Jiang, T. Qiu, Y. Meng and X. Li, *Polymer*, 2014, **55**, 4601–4610.
61 H. De Brouwer, M. A. J. Schellekens, B. Klumperman, M. J. Monteiro and A. L. German, *J. Polym. Sci., Part A: Polym. Chem.*, 2000, **38**, 3596–3603.
62 J. Liu, H. Duong, M. R. Whittaker, T. P. Davis and C. Boyer, *Macromol. Rapid Commun.*, 2012, **33**, 760–766.
63 A. Blanazs, R. Verber, O. O. Mykhaylyk, A. J. Ryan, J. Z. Heath, C. W. I. Douglas and S. P. Armes, *J. Am. Chem. Soc.*, 2012, **134**, 9741–9748.
64 C. W. Scales, E. R. George, C. D. Anderson, R. D. Gleim and B. M. Healy, *WO*, 2013085814-A2013085812, 2013.
65 K. L. Thompson, C. J. Mable, A. Cockram, N. J. Warren, V. J. Cunningham, E. R. Jones, R. Verber and S. P. Armes, *Soft Matter*, 2014, **10**, 8615–8626.
66 Y. X. Ma, X. L. Zheng, F. M. Shi, Y. Li and S. J. Sun, *J. Appl. Polym. Sci.*, 2003, **88**, 1622–1626.
67 J. Jang and B. S. Kim, *J. Appl. Polym. Sci.*, 2000, **77**, 903–913.
68 Y. Feng and C. F. Xiao, *J. Appl. Polym. Sci.*, 2006, **101**, 1248–1251.
69 Z. Janovic, K. Saric and K. Sertic-Bionda, *Chem. Biochem. Eng. Q.*, 1998, **12**, 19–24.
70 A. Jukic, E. Vidovic and Z. Janovic, *Chem. Technol. Fuels Oils*, 2007, **43**, 386–394.
71 R. L. Stambaugh and B. G. Kinker, *Viscosity Index Improvers and Thickeners*, Springer-Verlag Berlin, Berlin, 2010.
72 R. Zheng, G. Liu, M. Devlin, K. Hux and T.-C. Jao, *Tribol. Trans.*, 2010, **53**, 97–107.
73 R. Zheng, G. Liu and T.-C. Jao, *Polymer*, 2007, **48**, 7049–7057.
74 J. S. Trent, *Macromolecules*, 1984, **17**, 2930–2931.
75 Our previously reported protocol for TEM staining using RuO_4 (*Chem. Sci.*, **4**, 2081–2087 and *J. Am. Chem. Soc.*, 2014, **136**, 5790–5798) gave incorrect oxidation states. Those quoted in this manuscript are correct.
76 P. Cacioli, D. G. Hawthorne, R. L. Laslett, E. Rizzardo and D. H. Solomon, *J. Macromol. Sci., Chem.*, 1986, **23**, 839–852.
77 M. Rodlert, E. Harth, I. Rees and C. J. Hawker, *J. Polym. Sci., Part A: Polym. Chem.*, 2000, **38**, 4749–4763.
78 R. Verber, A. Blanazs and S. P. Armes, *Soft Matter*, 2012, **8**, 9915–9922.
79 J. van Stam, S. Creutz, F. C. De Schryver and R. Jérôme, *Macromolecules*, 2000, **33**, 6388–6395.